ACS MATERIALS LETTERS

www.acsmaterialsletters.org

Inverse Elastocaloric Output in Supramolecular Liquid Crystalline Elastomers

Mohsin Hassan Saeed, Jeremy A. Herman, Avijit Das, David T. Kennedy, and Timothy J. White*

Cite This: *ACS Materials Lett.* 2025, 7, 2688−2694

Read Online

ACCESS | Metrics & More | Article Recommendations | Supporting Information

ABSTRACT: Elastocaloric cooling is a promising solid-state alternative to vapor-compression refrigeration. In conventional systems, such as natural rubber, deformation induces entropy change accompanied by temperature release. Unloading the material restores the entropic state and is accompanied by cooling. Inverse elastocaloric effects have been detailed in shape memory alloys, where deformation induces loss of order and cooling. Here, we report on a distinctive inverse elastocaloric effect in liquid crystalline elastomers (LCEs) containing supramolecular hydrogen bonds. Upon deformation, the supramolecular LCE exhibits initial organization but then disorganizes as the intramesogenic hydrogen bonds are broken. Due to the liquid crystalline nature of the dimeric supramolecular bonds, the mechanochemical bond breakage manifests in a disruption in order. By disrupting the extent of liquid crystallinity in the system, we hypothesize that the network disorganizes to the deformation (e.g., entropy increases) and produces an inverse elastocaloric output.

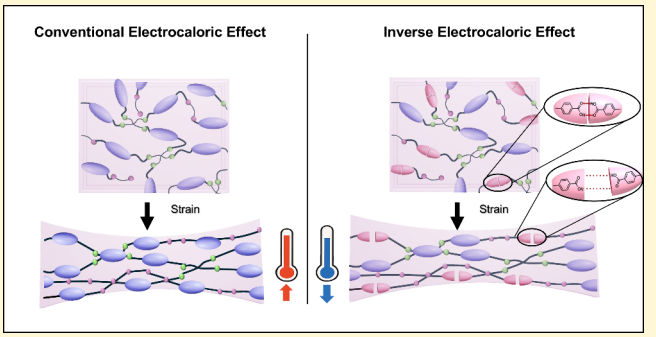

Liquid crystal elastomers (LCEs) are an important class of stimuli-responsive polymeric materials that combine the elastic properties of polymer networks with the anisotropic properties of liquid crystals (LCs).[1−5] This combination imparts LCEs with remarkable mechanical properties that can be accessed by external stimuli such as temperature, light, magnetic field, and electric field.[6,7] LCEs combine the molecular order of LCs and the entropic elasticity of the polymer matrix. The structural anisotropy is retained from liquid crystalline (e.g., mesogenic) monomer precursors.[8−10] The coupling between the molecular alignment of LCs and the macroscopic behavior of the polymer matrix allows LCEs to undergo significant, reversible deformations in response to small changes in external conditions.[11−16] The stimuli-responsive deformation makes LCEs highly attractive for applications in soft robotics,[17,18] actuators,[19−23] sensors,[24−27] and artificial muscles.[28−30]

The elastocaloric effect, a phenomenon where materials undergo heating or cooling due to mechanical deformation, has been observed in various systems, most notably in natural rubber and shape memory alloys (SMAs).[31−34] In natural rubber, stretching aligns polymer chains (strain-induced crystallization), reducing entropy and causing a temporary increase in temperature. Upon releasing the strain, the chains return to a disordered state, and the material cools.[34−36] In SMAs, the elastocaloric response is associated with stress-induced martensitic phase transitions, where structural rearrangements under load result in significant entropy changes and corresponding thermal effects. These materials have demonstrated promising applications in solid-state refrigeration technologies, offering energy-efficient alternatives to conventional vapor-compression cooling.[37,38] Recently, attention has turned to exploring other classes of materials such as shape memory polymers (SMPs) as well as LCEs.[38,39] These materials exhibit unique coupling between mechanical deformation and molecular ordering, providing exciting opportunities to explore and optimize elastocaloric performance for responsive, low-hysteresis, and cyclable cooling applications.

The elastocaloric effect in LCEs has been the focus of a few recent reports.[39,40] For LCE, the application of mechanical stress induces an isothermal decrease in the entropy and emission of heat. Mechanical deformation of conventional LCEs either can result in a mechanotropic phase transition[41,42] or cooperative organization of domains (e.g., polydomain to monodomain transition). Both mechanisms have been reported to result in temperature increases to deformation followed by cooling on release.[42] Several studies have demonstrated elastocaloric

Received: February 16, 2025
Revised: June 17, 2025
Accepted: June 18, 2025
Published: June 30, 2025

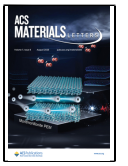

https://doi.org/10.1021/acsmaterialslett.5c00331
ACS Materials Lett. 2025, 7, 2688−2694

temperature changes in the range of 1−2 °C in polydomain LCEs under relatively low mechanical stress.[39] Computational predictions suggest even larger temperature changes can be realized with optimized composition and LC content of the material.[43] Recent reports have introduced the use of mechanotropic phase transitions in liquid-crystalline containing amorphous materials to produce moderate elastocaloric effects.[41,42] Thus, far, the attainable temperature change has reached ± 3.5 °C under minimal stress and strain with near-zero hysteresis which may position LCEs as promising candidates for practical elastocaloric applications.[44]

In addition to the conventional elastocaloric effect, where materials heat under strain and cool upon release, the inverse elastocaloric effect, typified by cooling under applied stress and heating upon relaxation, has been observed in shape memory alloys (SMAs)[43,45] with the associated thermodynamics of the inverse system attributable to stress induced increase in entropy that results in a concurrent decrease in temperature.[33] The Maxwell relation describing this effect is given by

$$\left(\frac{\partial s}{\partial \sigma}\right)_T = \left(\frac{\partial \varepsilon}{\partial T}\right)_\sigma$$

where S is entropy, σ is applied stress, ε is strain, and T is temperature. When $\left(\frac{\partial \varepsilon}{\partial T}\right)_\sigma > 0$, the material cools under stress due to an increase in entropy.[46] This behavior is observed during phase transitions that involve changes in symmetry but do not result in significant volume changes such as the martensitic transitions of some metal alloys. In these materials, the interplay between stress and strain governs the transformation, and significant entropy changes near the transition point can lead to substantial cooling effects.[47] In SMAs, the inverse effect arises due to the interplay between structural transformations and secondary phenomena such as internal stress fields or magnetism. For example, alloys such as Co−Cr−Al−Si have demonstrated inverse elastocaloric output associated with a reentrant martensitic phase transformation driven by magnetic interactions.[31,48]

While ultimately the design of an elastocaloric cooling system can use either a conventional or inverse elastocaloric material, we speculate that the realization of both effects in polymeric materials could be used in parallel or series in advanced designs. While prior examinations detail inverse elastocaloric effects in SMAs, we are unaware of any reports of inverse elastocaloric output in soft, polymeric systems. Accordingly, we report what we believe is a distinctive inverse elastocaloric output in supramolecular LCE. We demonstrate that stretching this new subset of LCEs disrupts the hydrogen bonds, which is an endothermic process involving a positive enthalpy change. The energy absorbed during bond disruption contributes to the observed cooling effect, as the system draws in heat to compensate for bond breaking. This cooling effect is accompanied by an increase in entropy resulting from the disruption of hydrogen bonds that compose the dimeric liquid crystal units in the LCE. Accordingly, deformation eventually reduces the order. The combined effect of enthalpy (heat absorption) and entropy (increased disorder) during deformation results in a temperature decrease with minimum applied stress. Furthermore, these elastomers rapidly recover to strain cycling due to their low nematic-to-isotropic transition temperatures (T_{NI}) and accordingly, exhibit minimal mechanical hysteresis.

The supramolecular LCE composition examined here were prepared via thiol−acrylate photopolymerization of liquid crystalline diacrylate monomers C6BAPE, the supramolecular monomer M_6OBA, and thiol-based cross-linker and chain extender (Figure 1a). M_6OBA dimerizes to form a liquid crystalline phase. Mixtures were filled at room temperature into glass substrates spaced by 100 μm spacers. Upon photopolymerization (Figure 1b), the polymer network forms and is composed of both covalent bonds and noncovalent bonds (via hydrogen bonding). Second heating curve of differential scanning calorimetry (DSC) analysis is presented in Figure 1c indicating that the glass transition temperature (T_g) is well below room temperature. The T_{NI} of this supramolecular LCE composition is around room temperature. These transitions were also observed during dynamic mechanical analysis (DMA) with a temperature ramp under dynamic oscillation at a frequency of 1 Hz (Figure S2). The maximum peak of the tan(δ) curve, representing T_g, appeared at ≈ −3 °C, while the other peak at ≈27 °C corresponded to T_{NI}.

The mechanical properties of the supramolecular LCE are evident in tensile testing (Figure 2a). With a near-ambient T_{NI}, the material deforms similar to the "isotropic" LCE subject to our recent examination.[44] The material exhibited elastic deformation with a modulus of 0.87 MPA. The supramolecular LCE was also examined for hysteresis and creep recovery. The material is fully reversible at room temperature (Figure S3). Infrared spectroscopy was used to assess the potential mechanochemical response of the supramolecular LCE. The LCE was deformed and placed on an ATR crystal. IR spectra were taken immediately. Although the material is soft and recovers rapidly due to minimal hysteresis, the samples were initially cooled to their T_g to immobilize the polymer network, and slow the time scale of recovery to enable spectral acquisition. Notably, the stretching is only up to 75%, the peak at 1680 cm^{-1} corresponding to the carbonyl stretch of dimerized M_6OBA decreases in height upon stretching is attributed to the disruption of hydrogen bonds (Figure 2b) within the supramolecular LCE network, which dilutes the liquid crystalline phases and leads to a uniform optical state.[49−52]

Previous studies of LCEs have established elastocaloric phenomena. When LCEs prepared of entirely covalent bonds are subjected to stress, the polymer network aligns, increasing its order, which causes an initial rise in temperature. As the material alignment saturates, the temperature increases causes heat (Q) to be lost to the environment, and the sample returns to the ambient temperature. Upon stress release, the material reverts back to the disordered state accompanied by a decrease in temperature.[42,44] This phenomenon is attributed to entropy changes. The transition from a disordered to an ordered state decreases entropy, leading to a temperature increase (exothermic), while the return to disorder upon unloading increases entropy, resulting in cooling (endothermic). The elastocaloric curve for a conventional LCE (e.g., entirely covalent) is shown in Figure S4.

The elastocaloric response of the supramolecular LCE was observed during deformation by thermal imaging (Figure 3a, Movie S1). Here, the material was subject to deformation at the strain rate of 16.67%/s to a value of 75% strain. Upon deformation, the material exhibits an initial −0.2 °C decrease in temperature. This decrease in temperature was repeatedly observed in replicate samples as well as in other related compositions. However, the magnitude of the temperature change was highly irregular affecting statistical analysis.

https://doi.org/10.1021/acsmaterialslett.5c00331
ACS Materials Lett. 2025, 7, 2688−2694

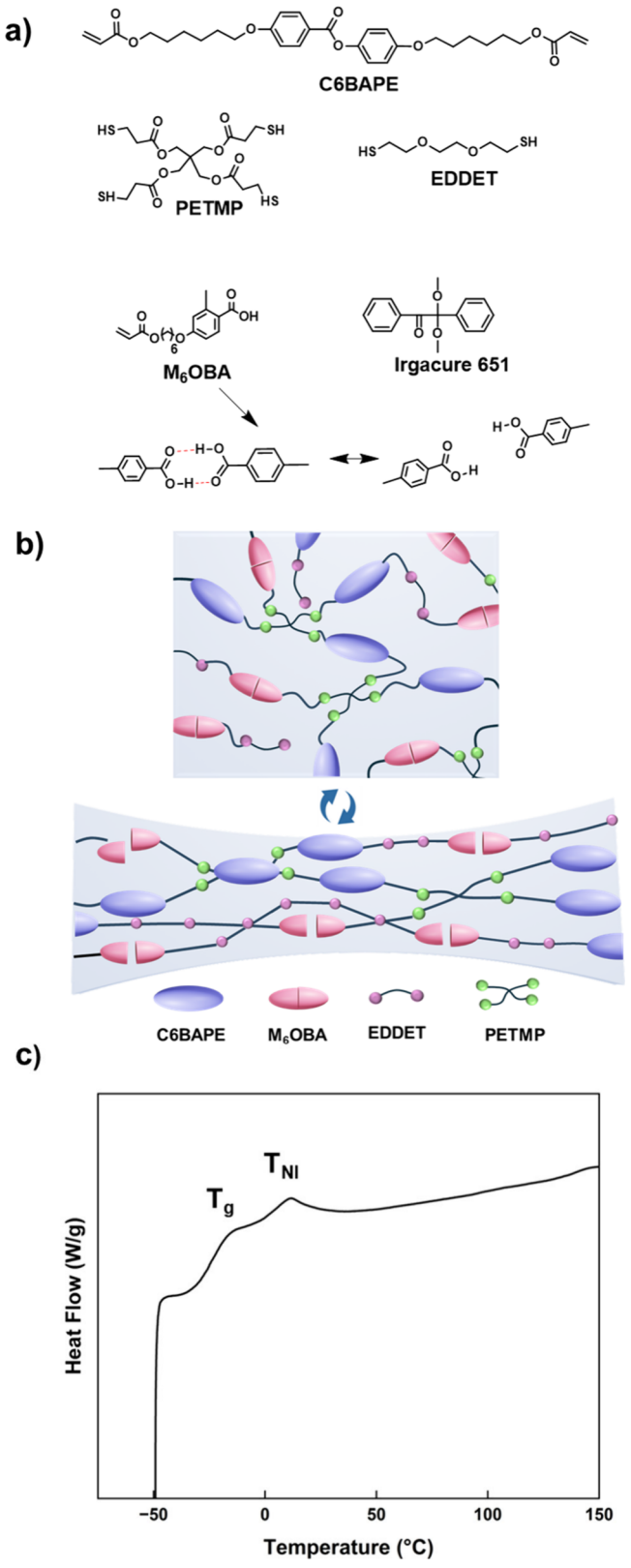

Figure 1. (a) Chemical structures of liquid crystalline diacrylate monomer C6BAPE, tetrathiol cross-linker (PETMP), dithiol chain extender (EDDET), supramolecular liquid crystalline monomers (M_6OBA), an illustration of a dimerized hydrogen bond, and photoinitiator (Irgacure 651). These monomers are subject to free-radical chain-transfer photopolymerization to produce the LCE. (b) Schematic representing polymer network containing covalent and noncovalent mesogenic units. Upon mechanical deformation the supramolecular mesogens M_6OBA reversibly cleaves at moderate strain values. (c) Second heating curve of differential scanning calorimetry (DSC) for supramolecular LCEs showing glass transition temperature (T_g) and nematic-to-isotropic transition temperature (T_{NI}) of the material.

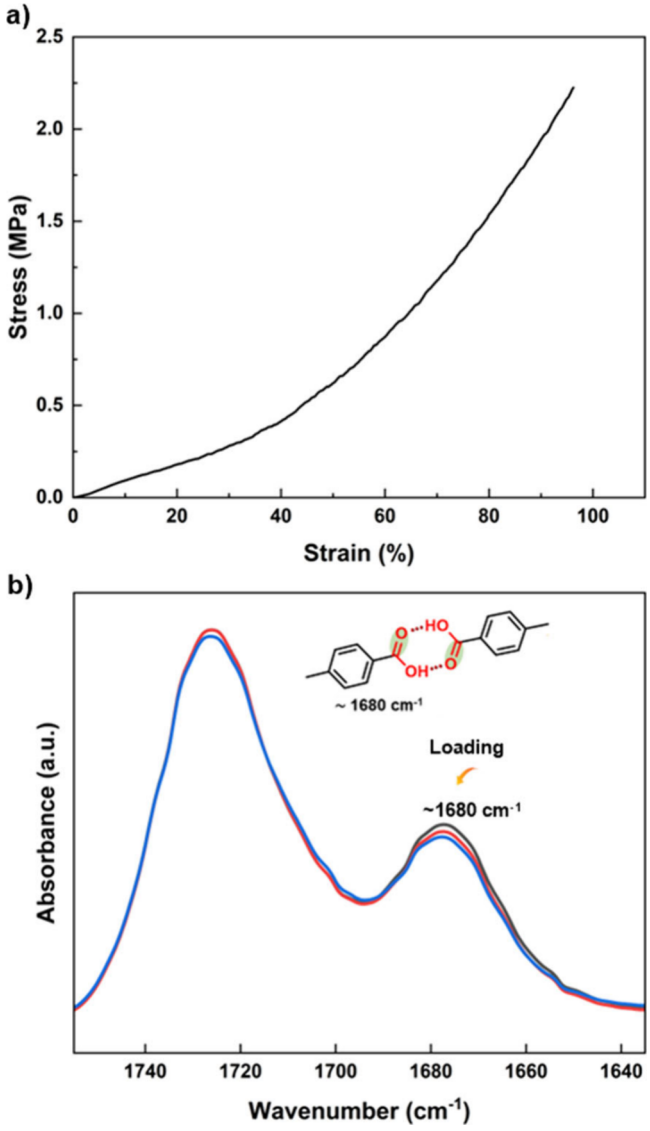

Figure 2. (a) Tensile deformation of LCEs from 0 to 100% strain at a rate of 10% min^{-1} (at room temperature). (b) Evidence of mechanochemical bond disruption of a deformed supramolecular LCE observed via ATR-IR spectra. The dimer peak at 1680 cm^{-1} exhibits a discernible decrease to load at this timepoint while the monomeric peak at 1730 cm^{-1} increases.

Accordingly, we choose to present a representative sample that illustrates the observation of the response. At maximum strain, the sample is held and the temperature further drops an additional −0.5 °C. The tensile deformation is released, and the material consistently exhibits a −0.1 °C decrease in temperature on release. The total temperature decrease on deformation in this sample was −0.7 °C. The evolution of strain and temperature as a function of time for this experiment is presented in Figure 3b. To ensure the reproducibility, we

https://doi.org/10.1021/acsmaterialslett.5c00331
ACS Materials Lett. 2025, 7, 2688−2694

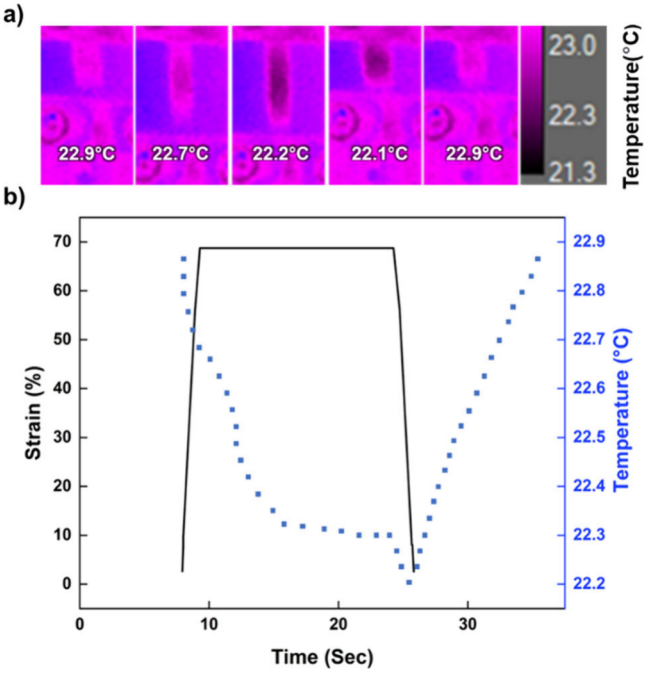

Figure 3. (a) FLIR images taken during the deformation of C6BAPE$_{37}$ MeOBA$_{32}$. The sample's average measured temperature (from the central region of the sample) is inset in each image. (b) The evolution of temperature is plotted as a function of time to deformation of the material to 75% strain at the rate of 16.67/s, held for 15 s, and then taken to 0% strain.

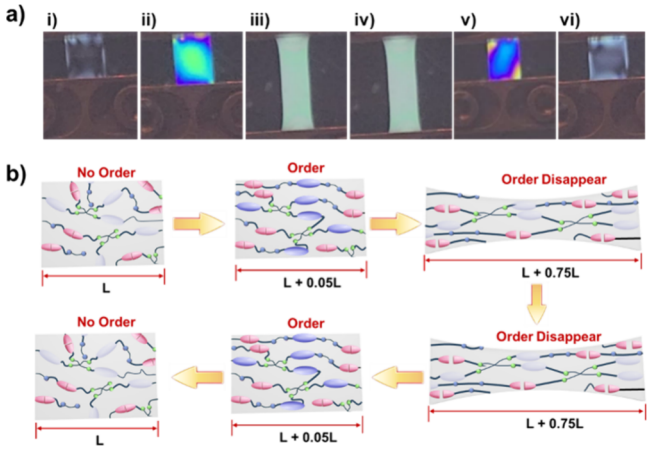

Figure 4. (a) Cross-polarized photographs of supramolecular LCE strained from 0 to 75% and recovery. (i) No order. (ii) Minimal deformation induces orientation in the network, corresponding to ordered mesogen domains (near-zero hydrogen bond breakage). (iii) The uniform optical appearance, as strain increased, during holding confirming hydrogen bond breakage. (iv) unloading, (v) recovery indicated reformation of hydrogen bonds and restoration of liquid crystalline order, vi) No order. b) Illustration summarizing the deformation mechanism of supramolecular Liquid crystalline elastomer: a) network of conventional and H-bonded mesogens, (b) minimum deformation induces orientation to this network (near zero H bond breakage) - classical polydomain to monodomain transition, and (c) further deformation starts to result in H-bond dissociation thereby diluting the liquid crystal (LC) order and surpassing the LC phase and also diluting the birefringence colors. It should be noted that the disruption of hydrogen bonds increases in entropy and thus a negative DT cycle. (d) During the holding step hydrogen bonds remain apart and entropy is increased and thus a more negative DT. (e) Recovery to the nematic state and reformation of H-bonds and the LC phase surpassing the hydrogen bonds and (f) force completely removed on the LCE and it is no order again.

conducted five repeated deformation−recovery cycles as shown in Figure S5.

Informed by IR analysis, we believe that a majority of the cooling is associated with mechanochemical disruption of the hydrogen bonds in the material. We were not able to deconflict the contribution of enthalpic disruption of the bonds versus the entropic contributions. However, for this particular material system, we note the rate dependence of the process. We do not observe the inverse elastocaloric effect to instantaneous (rapid) deformation to 75% shown in Figure S6. We speculate that the slow application of strain at 16.67%/s as well as the extended holding period allows for the force to be sustained in the material, which could enhance the amount of overcoming the energy barrier for dimerization. The effects of strain rate and stretching percentage are shown in Figure S7 and S8. Careful experimentation is necessary to elucidate the underlying mechanism in detail. However, the decrease in temperature aligns with our hypothesis that deformation of supramolecular LCE can disrupt hydrogen bonds within the LCE structure and ultimately result in an inverse elastocaloric effect. The contrast between the response of conventional and supramolecular LCEs is shown in Figure S9.

As an initial confirmation of the association of deformation of supramolecular LCE and order decrease, we utilized birefringent imaging between crossed polarizers (Figure 4a, Movie S2). With the proximity of T_{NI} to room temperature, the material is generally isotropic (initially lacks birefringence). Some birefringence is observed proximate to the grips. As strain is applied, the material becomes strongly birefringent. This indicates the material is exhibiting a classical mechanotropic phase transition (entropy decrease). However, to continued deformation the birefringence largely vanishes and the film exhibits a milky-white texture between crossed polarizers. This is indicative of some residual retention of order at a considerably reduced magnitude. This experiment supports the conclusion that deformation of the supramolecular LCE does affect organization (e.g., entropy increase). Upon unloading, the material once again becomes strongly birefringent before returning to a generally isotropic state. For comparison, photographs of a conventional LCE subject to a similar deformation cycle are shown in Figure S10.

From the data presented in Figure 3a and 3b, the deformation of these materials is consistent with prior examinations that refer to the inverse elastocaloric effect. However, the evolution of entropy in these materials is nuanced. The material begins in an isotropic state. Upon deformation, we propose the material transitions into a nematic phase. This is a decrease in entropy which should manifest as an increase in temperature. However, although this birefringent image is evident in the process, it is limited in time such that the emanation of heat in this state may be limited and not detectable with our methodology. Sustaining and eventually holding deformation results in hydrogen bond disruption. The exact amount of disruption is unclear. The mechanochemical disruption of hydrogen bonds is itself an endothermic process (cooling). However, birefringence measurements confirm changes in organization that suggest that the mechanically induced cooling is a combination of enthalpic and entropic components.

https://doi.org/10.1021/acsmaterialslett.5c00331
ACS Materials Lett. 2025, 7, 2688−2694

Notably, upon release, the elastocaloric process reported here does not exhibit a positive temperature change. Although initially counterintuitive, this may be indirect evidence of the contribution of the mechanotropic phase transition to the process in this particular material system. At the deformed state, the material clearly has a limited amount of order. When strain is released, the material is further cooled before the temperature returns to ambient. We speculate that the temperature drop on strain release, which is repeatedly seen in samples, is associated with the reverse mechanotropic process, where some amount of order is initially regained. The elastic recovery of the material is rapid (Figure S3b). The duration of the ordered state is limited in duration. The recovery in temperature may be a counterbalance of the exothermic nature of hydrogen bond reformation balanced with the entropic recovery of order and subsequent return to the isotropic state. A summary of the deformation and recovery processes is presented in Figure 4b.

This work reports the observation of inverse elastocaloric effect in supramolecular liquid crystalline elastomers (LCEs) composed of intramesogenic hydrogen bonds. The inverse elastocaloric response of the LCE is associated with mechanochemical dissociation of the hydrogen bonds. Thermodynamically, the mechanically induced order−disorder transition increases entropy and manifests as cooling. In this initial report, the elastocaloric output is < −1 °C. These findings establish a foundation for tuning LCE properties through supramolecular design, enabling highly responsive, low-hysteresis, and cyclable caloric materials capable of inverse elastocaloric response.

■ ASSOCIATED CONTENT

Supporting Information

The Supporting Information is available free of charge at https://pubs.acs.org/doi/10.1021/acsmaterialslett.5c00331.

Experimental section which includes: materials information, synthesis of M_6OBA, thermal and mechanical analysis, elastocaloric measurement and attenuated total reflectance infrared spectroscopy. Supporting Figures include tan (delta) curve, hysteresis and creep recovery, and conventional elastocaloric curve as well as schematic illustration of elastocaloric cycle for conventional and supramolecular LCE. Further, cross-polarized photographs of traditional LCE are provided for illustration (PDF)

Movie of the real-time temperature change observed by FLIR camera for supramolecular LCE (MP4)

Movie of the birefringence changes of supramolecular LCE under cross polarizers are also available (MP4)

■ AUTHOR INFORMATION

Corresponding Author

Timothy J. White − *Department of Chemical and Biological Engineering and Materials Science and Engineering Program, University of Colorado, Boulder, Colorado 80309, United States*; orcid.org/0000-0001-8006-7173; Email: tim.white@colorado.edu

Authors

Mohsin Hassan Saeed − *Department of Chemical and Biological Engineering, University of Colorado, Boulder, Colorado 80309, United States*

Jeremy A. Herman − *Department of Chemical and Biological Engineering, University of Colorado, Boulder, Colorado 80309, United States*

Avijit Das − *Department of Chemical and Biological Engineering, University of Colorado, Boulder, Colorado 80309, United States*

David T. Kennedy − *Department of Chemical and Biological Engineering, University of Colorado, Boulder, Colorado 80309, United States*

Complete contact information is available at: https://pubs.acs.org/10.1021/acsmaterialslett.5c00331

Author Contributions

The manuscript was written through contributions of all authors. M.H.S. prepared the materials and undertook inverse elastocaloric measurements. J.A.H. assisted with experiment setup and consulted on data analysis. A.D. undertook mechanical property measurements and assisted with illustration. D.T.K. synthesized and characterized the M_6OBA monomer. T.J.W. supervised the project. All authors have given approval to the final version of the manuscript.

Funding

The authors acknowledge support from the Petroleum Research Fund (M.H.S., T.J.W.), Army Research Office (M.H.S., T.J.W.), Graduate Research Fellowship of the National Science Foundation (J.A.H.), Air Force Office of Scientific Research (A.D., T.J.W.), and National Science Foundation (D.J.K., T.J.W.).

Notes

The authors declare no competing financial interest.

■ ACKNOWLEDGMENTS

We dedicate this contribution to the memory of Dritika Das who tragically passed away during this research activity.

■ REFERENCES

(1) White, T. J.; Broer, D. J. Programmable and Adaptive Mechanics with Liquid Crystal Polymer Networks and Elastomers. *Nat. Mater.* **2015**, *14*, 1087−1098.

(2) Herbert, K. M.; Fowler, H. E.; McCracken, J. M.; Schlafmann, K. R.; Koch, J. A.; White, T. J. Synthesis and Alignment of Liquid Crystalline Elastomers. *Nat. Rev. Mater.* **2022**, *7*, 23−38.

(3) Jiang, Z.-C.; Liu, Q.; Xiao, Y.-Y.; Zhao, Y. Liquid Crystal Elastomers for Actuation: A Perspective on Structure-Property-Function Relation. *Prog. Polym. Sci.* **2024**, *153*, 101829−101850.

(4) Sánchez-Ferrer, A.; Finkelmann, H. Thermal and Mechanical Properties of New Main-Chain Liquid-Crystalline Elastomers. *Mol. Cryst. Liq. Cryst.* **2009**, *508*, 348−356.

(5) Annapooranan, R.; Wang, Y.; Cai, S. Harnessing Soft Elasticity of Liquid Crystal Elastomers to Achieve Low Voltage Driven Actuation. *Adv. Mater. Technol.* **2023**, *8*, 2201969−2201975.

(6) Javed, M.; Corazao, T.; Saed, M. O.; Ambulo, C. P.; Li, Y.; Kessler, M. R.; Ware, T. H. Programmable Shape Change in Semicrystalline Liquid Crystal Elastomers. *ACS Appl. Mater. Interfaces* **2022**, *14*, 35087−35096.

(7) Ma, J.; Yang, Y.; Valenzuela, C.; Zhang, X.; Wang, L.; Feng, W. Mechanochromic, Shape-Programmable and Self-Healable Cholesteric Liquid Crystal Elastomers Enabled by Dynamic Covalent Boronic Ester Bonds. *Angew. Chem., Int. Ed.* **2022**, *61*, 1−10.

(8) Saed, M. O.; Gablier, A.; Terentjev, E. M. Exchangeable Liquid Crystalline Elastomers and Their Applications. *Chem. Rev.* **2022**, *122*, 4927−4945.

(9) Skillin, N. P.; Bauman, G. E.; Kirkpatrick, B. E.; McCracken, J. M.; Park, K.; Vaia, R. A.; Anseth, K. S.; White, T. J. Photothermal Actuation

of Thick 3D-Printed Liquid Crystalline Elastomer Nanocomposites. *Adv. Mater.* **2024**, *36*, 1−11.
(10) Pranda, P. A.; Hedegaard, A.; Kim, H.; Clapper, J.; Nelson, E.; Hines, L.; Hayward, R. C.; White, T. J. Directional Adhesion of Monodomain Liquid Crystalline Elastomers. *ACS Appl. Mater. Interfaces* **2024**, *16*, 6394−6402.
(11) Yoon, H. H.; Kim, D. Y.; Jeong, K. U.; Ahn, S. K. Surface Aligned Main-Chain Liquid Crystalline Elastomers: Tailored Properties by the Choice of Amine Chain Extenders. *Macromolecules* **2018**, *51*, 1141−1149.
(12) Hebner, T. S.; Korner, K.; Bowman, C. N.; Bhattacharya, K.; White, T. J. Leaping Liquid Crystal Elastomers. *Sci. Adv.* **2023**, *9*, 1−8.
(13) Ware, T. H.; McConney, M. E.; Wie, J. J.; Tondiglia, V. P.; White, T. J. Voxelated Liquid Crystal Elastomers. *Science (1979)* **2015**, *347*, 982−984.
(14) Feng, C.; Rajapaksha, C. P. H.; Cedillo, J. M.; Piedrahita, C.; Cao, J.; Kaphle, V.; Lüssem, B.; Kyu, T.; Jákli, A. Electroresponsive Ionic Liquid Crystal Elastomers. *Macromol. Rapid Commun.* **2019**, *40*, 1−8.
(15) Saed, M. O.; Elmadih, W.; Terentjev, A.; Chronopoulos, D.; Williamson, D.; Terentjev, E. M. Impact Damping and Vibration Attenuation in Nematic Liquid Crystal Elastomers. *Nat. Commun.* **2021**, *12*, 6676−6673.
(16) Herman, J. A.; Hoang, J. D.; McCracken, J. M.; White, T. J. Compositional and Temperature Dependence of Amorphous Polymer Networks Undergoing Mechanotropic Phase Transitions. *Macromolecules* **2024**, *57*, 664−671.
(17) Escobar, M. C.; White, T. J. Fast and Slow-Twitch Actuation via Twisted Liquid Crystal Elastomer Fibers. *Adv. Mater.* **2024**, *36*, 1−8.
(18) Sun, D.; Zhang, J.; Li, H.; Shi, Z.; Meng, Q.; Liu, S.; Chen, J.; Liu, X. Toward Application of Liquid Crystalline Elastomer for Smart Robotics: State of the Art and Challenges. *Polymers (Basel)* **2021**, *13*, 1889−1899.
(19) Saeed, M. H.; Choi, M. Y.; Kim, K.; Lee, J. H.; Kim, K.; Kim, D.; Kim, S. U.; Kim, H.; Ahn, S. K.; Lan, R.; Na, J. H. Electrostatically Powered Multimode Liquid Crystalline Elastomer Actuators. *ACS Appl. Mater. Interfaces* **2023**, *15*, 56285−56292.
(20) Phillips, A. T.; Schlafmann, K. R.; Fowler, H. E.; White, T. J. Electrically Tunable, Fully Solid Reflective Optical Elements. *Adv. Opt Mater.* **2022**, *10*, 1−10.
(21) Phillips, A. T.; Chen, J. C.; McCracken, J. M.; White, T. J. Dynamic Infrared Reflective Filters Prepared from Cholesteric Liquid Crystalline Elastomers. *ACS Applied Optical Materials* **2024**, *2*, 2559−2567.
(22) Nasare, R.; Guo, H.; Priimagi, A. Hydrogen-Bonded Multi-Mode Liquid Crystal Elastomer Actuators. *J. Mater. Chem. B* **2025**, *0*, 1−7.
(23) Lv, P.; Yang, X.; Bisoyi, H. K.; Zeng, H.; Zhang, X.; Chen, Y.; Xue, P.; Shi, S.; Priimagi, A.; Wang, L.; Feng, W.; Li, Q. Stimulus-Driven Liquid Metal and Liquid Crystal Network Actuators for Programmable Soft Robotics. *Mater. Horiz* **2021**, *8*, 2475−2484.
(24) Ohm, C.; Brehmer, M.; Zentel, R. Liquid Crystalline Elastomers as Actuators and Sensors. *Adv. Mater.* **2010**, *22*, 3366−3387.
(25) Han, W. C.; Lee, Y. J.; Kim, S. U.; Lee, H. J.; Kim, Y. S.; Kim, D. S. Versatile Mechanochromic Sensor Based on Highly Stretchable Chiral Liquid Crystalline Elastomer. *Small* **2023**, *19*, 2206299−2206306.
(26) Li, S.; Bai, H.; Liu, Z.; Zhang, X.; Huang, C.; Wiesner, L. W.; Silberstein, M.; Shepherd, R. F. Digital Light Processing of Liquid Crystal Elastomers for Self-Sensing Artificial Muscles. *Sci. Adv.* **2021**, *7*, 3677−3700.
(27) Khan, M.; Li, W.; Hu, Q.; Lin, J.; Lin, L. Non-Invasive Ammonia Detection on Cancer Cell Surfaces Using Liquid Crystal Elastomer. *Adv. Mater. Technol.* **2024**, *0*, 1−10.
(28) Thomsen, D. L.; Keller, P.; Naciri, J.; Pink, R.; Jeon, H.; Shenoy, D.; Ratna, B. R. Liquid Crystal Elastomers with Mechanical Properties of a Muscle. *Macromolecules* **2001**, *34*, 5868−5875.
(29) Sun, J.; Wang, Y.; Liao, W.; Yang, Z. Ultrafast, High-Contractile Electrothermal-Driven Liquid Crystal Elastomer Fibers towards Artificial Muscles. *Small* **2021**, *17*, 1−9.
(30) Lee, J.; Bae, J.; Hwang, J. H.; Choi, M.; Kim, Y. S.; Park, S.; Na, J.; Kim, D.; Ahn, S. Robust and Reprocessable Artificial Muscles Based on Liquid Crystal Elastomers with Dynamic Thiourea Bonds. *Adv. Funct Mater.* **2022**, *32*, 1−10.
(31) Xiao, F.; Li, Z.; Chen, H.; Jin, X.; Planes, A.; Fukuda, T. Origin of the Inverse Elastocaloric Effect in a Ni-Rich Ti-Ni Shape Memory Alloy Induced by Oriented Nanoprecipitates. *Phys. Rev. Mater.* **2021**, *5*, 53603−53609.
(32) Villa, E.; Villa, F.; Crespo, B. R.; Lazpita, P.; Salazar, D.; Hosoda, H.; Chernenko, V. Shape Memory and Elastocaloric Properties of Melt-Spun NiMn-Based Heusler Alloys. *J. Alloys Compd.* **2023**, *965*, 171437−171445.
(33) Yu, C.; Zhou, T.; Kan, Q.; Kang, G.; Fang, D. A Two-Scale Thermo-Mechanically Coupled Model for Anomalous Martensite Transformation and Elastocaloric Switching Effect of Shape Memory Alloy. *J. Mech Phys. Solids* **2022**, *164*, 104893−104901.
(34) Zhang, S.; Fu, Y.; Li, C.; Nie, X.; Chen, J.; Zhou, Y.; Ye, Z.; Zhou, X.; Shu, B.; Xiong, C.; Yang, Q.; Wang, Q. Polymer Elastomer near Plastic-to-Rubber Critical Transition Produces Enhanced Elastocaloric Effects. *Cell Rep. Phys. Sci.* **2022**, *3*, 101147−101160.
(35) Wang, K.; Engelbrecht, K.; Bahl, C. R. H. Additive Manufactured Thermoplastic Elastomers for Low-Stress Driven Elastocaloric Cooling. *Appl. Mater. Today* **2023**, *30*, 101711−101724.
(36) Sebald, G.; Lombardi, G.; Coativy, G.; Jay, J.; Lebrun, L.; Komiya, A. High-Performance Polymer-Based Regenerative Elastocaloric Cooler. *Appl. Therm Eng.* **2023**, *223*, 120016−120030.
(37) Qian, S.; Catalini, D.; Muehlbauer, J.; Liu, B.; Mevada, H.; Hou, H.; Hwang, Y.; Radermacher, R.; Takeuchi, I. High-Performance Multimode Elastocaloric Cooling System. *Science (1979)* **2023**, *380*, 722−727.
(38) Hartquist, C. M.; Lin, S.; Zhang, J. H.; Wang, S.; Rubinstein, M.; Zhao, X. An Elastomer with Ultrahigh Strain-Induced Crystallization. *Sci. Adv.* **2023**, *9*, 1−10.
(39) Lavrič, M.; Derets, N.; Črešnar, D.; Cresta, V.; Domenici, V.; Rešetič, A.; Skačej, G.; Sluban, M.; Umek, P.; Zalar, B.; Kutnjak, Z.; Rožič, B. Tunability of the Elastocaloric Response in Main-Chain Liquid Crystalline Elastomers. *Liq Cryst.* **2021**, *48*, 405−411.
(40) Skačej, G. Elastocaloric Effect in Liquid Crystal Elastomers from Molecular Simulations. *Liq Cryst.* **2018**, *45*, 1964−1969.
(41) Trèek, M.; Lavriè, M.; Cordoyiannis, G.; Zalar, B.; Rožič, B.; Kralj, S.; Tzitzios, V.; Nounesis, G.; Kutnjak, Z. Electrocaloric and Elastocaloric Effects in Soft Materials. *Philosophical Transactions of the Royal Society A: Mathematical, Physical and Engineering Sciences* **2016**, *374*, 20150301−20150312.
(42) Koch, J. A.; Herman, J. A.; White, T. J. Elastocaloric Effect in Amorphous Polymer Networks Undergoing Mechanotropic Phase Transitions. *Phys. Rev. Mater.* **2021**, *5*, 1−6.
(43) Črešnar, D.; Rožič, B.; Kutnjak, Z.; Kralj, S. Theoretical and Experimental Study of Elastocaloric Responses in Liquid Crystalline Elastomers. *J. Mol. Liq.* **2024**, *413*, 126058.
(44) Herman, J. A.; Hoang, J. D.; White, T. J. Elastocaloric Response of Isotropic Liquid Crystalline Elastomers. *Small* **2024**, *20*, 1−9.
(45) Črešnar, D.; Derets, N.; Trček, M.; Skačej, G.; Rešetič, A.; Lavrič, M.; Domenici, V.; Zalar, B.; Kralj, S.; Kutnjak, Z.; Rožič, B. Caloric Effects in Liquid Crystal-Based Soft Materials. *Journal of Physics: Energy* **2023**, *5*, 045004−045017.
(46) Mañosa, L.; Planes, A. Elastocaloric Effect in Shape-Memory Alloys. *Shape Memory and Superelasticity* **2024**, *10*, 89−98.
(47) Xiao, F.; Fukuda, T.; Kakeshita, T. Inverse Elastocaloric Effect in a Ti-Ni Alloy Containing Aligned Coherent Particles of Ti3Ni4. *Scr Mater.* **2016**, *124*, 133−137.
(48) Odaira, T.; Xu, S.; Xu, X.; Omori, T.; Kainuma, R. Elastocaloric Switching Effect Induced by Reentrant Martensitic Transformation. *Appl. Phys. Rev.* **2020**, *7*, 1−11.
(49) Lewis, K. L.; Herbert, K. M.; Matavulj, V. M.; Hoang, J. D.; Ellison, E. T.; Bauman, G. E.; Herman, J. A.; White, T. J. Programming Orientation in Liquid Crystalline Elastomers Prepared with Intra-Mesogenic Supramolecular Bonds. *ACS Appl. Mater. Interfaces* **2023**, *15*, 3467−3475.

https://doi.org/10.1021/acsmaterialslett.5c00331
ACS Materials Lett. 2025, 7, 2688−2694

(50) Lewis, K. L.; Hoang, J. D.; Toney, M. F.; White, T. J. Order-Disorder Transition of Supramolecular Liquid Crystalline Elastomers. *Chem. Mater.* **2025**, *37*, 175−188.
(51) Giubertoni, G.; Hilbers, M.; Caporaletti, F.; Laity, P.; Groen, H.; Van der Weide, A.; Bonn, D.; Woutersen, S. Hydrogen Bonds under Stress: Strain-Induced Structural Changes in Polyurethane Revealed by Rheological Two-Dimensional Infrared Spectroscopy. *J. Phys. Chem. Lett.* **2023**, *14*, 940−946.
(52) Kato, T.; Fréchet, J. M. J. Stabilization of a Liquid-Crystalline Phase through Noncovalent Interaction with a Polymer Chain. *Macromolecules* **1989**, *22*, 3818−3821.

https://doi.org/10.1021/acsmaterialslett.5c00331
ACS Materials Lett. 2025, 7, 2688−2694